Applied Bionics and Biomechanics 11 (2014) 69–79
DOI 10.3233/ABB-140087
IOS Press

Effect of slip on peristaltic flow of Powell-Eyring fluid in a symmetric channel

T. Hayat[a,b,*], S. Irfan Shah[a], B. Ahmad[b] and M. Mustafa[c]
[a]*Department of Mathematics, Quaid-I-Azam University, Islamabad, Pakistan*
[b]*Department of Electrical and Computer Engineering, Faculty of Engineering, King Abdulaziz University, Jeddah, Saudi Arabia*
[c]*School of Natural Sciences, National University of Sciences and Technology (NUST), Islamabad, Pakistan*

Abstract. Peristaltic flow of non-Newtonian fluid in a symmetric channel with partial slip effect is examined. The non-Newtonian behavior of fluid is characterized by the constitutive equations of Powell-Eyring fluid. The motion is induced by a sinusoidal wave traveling along the flexible walls of channel. The flow is analyzed in a wave frame of reference moving with the velocity of wave. The equations governing the flow are solved by adopting lubrication approach. Series solutions for the stream function and axial pressure gradient are obtained. Impact of slip and other emerging flow parameters is plotted and analyzed graphically.

1. Introduction

The mechanism of pumping fluid in channel/tube from a region of lower pressure to higher one is known as peristalsis. Peristaltic phenomenon is unique in the sense that fluid is transported by the action of a progressive sinusoidal wave of area contraction or expansion that propagates along the length of an extensible tube/channel instead of using piston. Peristaltic flow of Newtonian and non-Newtonian fluids has been widely recognized by several investigators due its extensive physiological and engineering applications. In physiology the peristalsis occurs in swallowing food through esophagus, chyme movement in the gastrointestinal tract, urine transport from kidney to bladder through the ureter, vasomotion of blood vessels in capillaries and arterioles. The transport of corrosive fluid, sanitary fluid, slurries and naxious fluid in the nuclear industry is also because of peristaltic pumping. Furthermore blood pumps in heart lung machine and roller and finger pumps also operate on the principle of peristaltic pumping. The earliest study obout the mechanism of peristaltic transport of viscous fluid was carried out by Latham [1]. Shapiro et al. [2] presented a mathematical model for peristaltic pumping under the assumptions of long wavelength and low Reynolds number approximation. He considered the flow of viscous fluid in a two-dimensional channel. In this study, the authors analyzed peristaltic pumping reflux and trapping. Afterwards several analytical, numerical and experimental studies related to peristaltic flows have been reported under different flow geometries and assumptions. Some useful attempts in this direction can be consulted by the studies [3–12]. The analysis in all these attempts has been made by employing no-slip boundary conditions and one or more simplified assumptions of long wavelength, low Reynolds number, small wave number, small amplitude ratio etc. Few useful contributions for MHD flows can be mentioned in the studies [13–15].

In many practical problems like polymeric liquids with higher molecular weights, problems of thin film, flow on multiple interface and problems of rare field

*Corresponding author: T. Hayat, Tel.: +92 51 90642172, Fax: +92 51 2601171. Email: pensy_t@yahoo.com.

fluid the fluid particle adjacent to a solid surface slip or stick-slip on solid boundaries and there is a relative motion between the fluid particles and solid wall due to which no-slip boundary condition is no-longer valid. Some theoretical and experimental investigations have been made on the peristaltic flow of viscous Newtonian and non-Newtonian fluids using partial slip condition. For instance Ali et al. [16] analyzed the peristaltic flow of MHD viscous fluid in a two-dimensional channel with variable viscosity and slip condition. The influence of slip condition, wall properties and heat transfer in MHD peristaltic transport of viscous fluid in a non-uniform channel has been studied by Srinivas et al. [17]. Here viscous fluid saturates the porous medium. Yildirm and Sezer [18] analyzed the effect of partial slip on the peristaltic flow of magnetohydrodynamic viscous fluid in an asymmetric channel. Hayat et al. [19] examined the influence of slip condition on the peristaltic transport in an asymmetric channel with heat transfer. Tripathi et al. [20] investigated the peristaltic transport of viscoelastic fractional Burgers' fluid under the influence of wall slip condition. Peristaltic flow of Williamson fluid in an inclined asymmetric channel with partial slip and heat transfer is analyzed by Akbar et al. [21]. Afsar et al. [22] studied the effect of variable viscosity on the peristaltic flow of non-Newtonian fluid through a porous medium with slip effect. Hayat and Mehmood [23] discussed the effect of slip on MHD peristaltic flow of third order fluid in a planar channel. Combined influence of velocity slip, temperature and concentration jump in MHD peristaltic transport of Carreau fluid in a non-uniform channel has been investigated by Vajravelu et al. [24].

The objective of present investigation is to analyze the effect of partial slip on peristaltic flow of non-Newtonian fluid in a symmetric channel. The proposed non-linear slip condition is dependent upon the shear stress. The non-Newtonian behavior of the fluid is characterized by the constitutive equations of Powell-Eyring fluid model. Powell-Eyring fluid model [25–28] is mathematically more complex and deserves attention due to the fact that its stress constitutive relation is deduced from kinetic theory of liquids rather than the empirical relation as in the case of power-law model. It also correctly reduces to Newtonian model for high shear rate. It is also worthmentioning that such study has not been already reported due to complexity of this fluid model. The current work has been carried out by employing lubrication approximation. Regular perturbation method is used to solve the problem. The layout of the study is organized as follows. In section two, the governing equations for the flow are modeled and presented under long wavelength approximation. Section three contains the series solutions for the stream function and axial pressure gradient. Section four synthesis the result and discussion for emerging parameters on the flow quantities of interest.

2. Mathematical formulation and modeling

We consider the flow of Powell-Eyring fluid in two-dimensional symmetric channel of width $2d$. The flow is induced by a sinusoidal peristaltic wave of small amplitude that travels along the flexible wall of channel. Flow analysis is carried out in a cartesian coordinate system when $\overline{X}$-axis lies along the central line of the channel and $\overline{Y}$-axis normal to it. The wall geometry due to the infinite train of peristaltic wave can be written as follows:

$$\overline{H}\left(\overline{X},\bar{t}\right) = d + b\sin\frac{2\pi}{\lambda}\left(\overline{X} - c\bar{t}\right), \tag{1}$$

in which b is the wave amplitude, d represents the mean half width of the channel, λ is the wavelength, c is the velocity of the peristaltic wave and $\bar{t}$ is the time.

The basic equations governing the flow of an incompressible fluid in the absence of body forces are

$$\mathrm{div}\bar{\mathbf{V}} = 0, \tag{2}$$

$$\rho\frac{d\bar{\mathbf{V}}}{d\bar{t}} = \mathrm{div}\overline{\mathbf{T}}, \tag{3}$$

where $d/d\bar{t}$ signifies the material derivative, ρ the density and $\bar{\mathbf{V}} = \{\bar{U}(\bar{X},\bar{Y},\bar{t}), \bar{V}(\bar{X},\bar{Y},\bar{t}), 0\}$ is the velocity of fluid. The expression of Cauchy stress tensor $\overline{\mathbf{T}}$ is

$$\overline{\mathbf{T}} = -\overline{p}\overline{\mathbf{I}} + \overline{\mathbf{S}}. \tag{4}$$

Here $\overline{p}$ is a pressure, $\overline{\mathbf{I}}$ the identity tensor and the extra stress tensor $\overline{\mathbf{S}}$ for a Powell-Eyring fluid is given by [25–28]:

$$\overline{\mathbf{S}} = \mu\left(\nabla\bar{\mathbf{V}}\right) + \frac{1}{\varpi}\sinh^{-1}\left(\frac{\nabla\bar{\mathbf{V}}}{\zeta}\right), \tag{5}$$

where μ is the dynamic viscosity and ϖ and ζ are the material constants of Powell-Eyring fluid. For the stress components the function is approximated as

$$\sinh^{-1}\left(\frac{\nabla\bar{\mathbf{V}}}{\zeta}\right)=\frac{\nabla\bar{\mathbf{V}}}{\zeta}-\left(\frac{\nabla\bar{\mathbf{V}}}{6\zeta}\right)^3 \text{ for } \left|\frac{\nabla\bar{\mathbf{V}}}{\zeta}\right|<<1. \tag{6}$$

Equations (2) and (3) through Equations (4 − 6) give

$$\overline{U}_{\overline{X}}+\overline{V}_{\overline{Y}}=0, \tag{7}$$

$$\rho(\bar{U}_{\bar{t}}+\overline{U}\bar{U}_{\overline{X}}+\overline{V}\bar{U}_{\overline{Y}})=-\bar{p}_{\overline{X}}+\left(\overline{S}_{\overline{XX}}\right)_{\bar{X}}+\left(\overline{S}_{\overline{XY}}\right)_{\bar{Y}}, \tag{8}$$

$$\rho(\overline{V}_{\bar{t}}+\overline{U}\overline{V}_{\overline{X}}+\overline{V}\overline{V}_{\overline{Y}})=-\bar{p}_{\overline{Y}}+\left(\overline{S}_{\overline{YX}}\right)_{\bar{X}}+\left(\overline{S}_{\overline{YY}}\right)_{\bar{Y}}, \tag{9}$$

$$\overline{S}_{\overline{XX}}=2\left(\mu+\frac{1}{\varpi\zeta}\right)\overline{U}_{\overline{X}}-\frac{1}{3\varpi\zeta^3}\left[2(\overline{U}_{\overline{X}})^3 +\overline{U}_{\overline{X}}(\overline{U}_{\overline{Y}}+\overline{V}_{\overline{X}})^2+2\overline{U}_{\overline{X}}(\overline{V}_{\overline{Y}})^2\right], \tag{10}$$

$$\overline{S}_{\overline{XY}}=2\left(\mu+\frac{1}{\varpi\zeta}\right)(\overline{U}_{\overline{Y}}+\overline{V}_{\overline{X}}) -\frac{1}{6\varpi\zeta^3}\left[\begin{array}{c}\{2(\overline{U}_{\overline{X}})^2+(\overline{U}_{\overline{Y}}+\overline{V}_{\overline{X}})^2\\ +2(\overline{V}_{\overline{Y}})^2\}(\overline{U}_{\overline{Y}}+\overline{V}_{\overline{X}})\end{array}\right], \tag{11}$$

$$\overline{S}_{\overline{YY}}=2\left(\mu+\frac{1}{\varpi\zeta}\right)\overline{V}_{\overline{Y}}-\frac{1}{3\varpi\zeta^3}\left[2\overline{V}_{\overline{Y}}(\overline{U}_{\overline{X}})^2 +\overline{V}_{\overline{Y}}(\overline{U}_{\overline{Y}}+\overline{V}_{\overline{X}})^2+2(\overline{V}_{\overline{Y}})^3\right], \tag{12}$$

where the subscripts denote the partial derivatives. Note that in the fixed coordinate system $(\overline{X},\overline{Y},\bar{t})$, the motion is time-dependent. However in a coordinate system $(\bar{x},\bar{y})$ moving with the wave speed c in the positive $\bar{x}$ direction the boundary shape is stationary. Defining the transformations

$$\bar{x}=\overline{X}-c\bar{t},\qquad \bar{y}=\overline{Y},\qquad \bar{u}=\overline{U}-c,\qquad \bar{v}=\overline{V} \tag{13}$$

and introducing the dimensionless variables

$$x=\frac{2\pi\bar{x}}{\lambda},\ y=\frac{\bar{y}}{d},\ u=\frac{\bar{u}}{c},\ v=\frac{\bar{v}}{c},$$
$$h(x)=\frac{\overline{H}(\bar{x})}{d},\ p=\frac{2\pi d^2}{\lambda\mu c}\bar{p},\ \delta=\frac{2\pi d}{\lambda},$$
$$S=\frac{d}{\mu c}\overline{S},\quad \mathrm{Re}=\frac{\rho c d}{\mu}\quad W=\frac{1}{\mu\varpi\zeta},\quad A=\frac{W}{6}\left(\frac{c}{\zeta d}\right)^2, \tag{14}$$

the resulting flow equations in terms of stream function $\Psi\left(u=\frac{\partial\Psi}{\partial y},\ v=-\delta\frac{\partial\Psi}{\partial x}\right)$ under lubrication approximations yield [16–20, 24]:

$$\frac{dp}{dx}=(1+W)\frac{\partial^3\Psi}{\partial y^3}-A\frac{\partial}{\partial y}\left(\frac{\partial^2\Psi}{\partial y^2}\right)^3, \tag{15}$$

$$S_{xy}=(1+W)\frac{\partial^2\Psi}{\partial y^2}-A\left(\frac{\partial^2\Psi}{\partial y^2}\right)^3, \tag{16}$$

$$(1+W)\frac{\partial^4\Psi}{\partial y^4}=A\frac{\partial^2}{\partial y^2}\left(\frac{\partial^2\Psi}{\partial y^2}\right)^3, \tag{17}$$

$$S_{xx}=S_{yy}=\frac{\partial p}{\partial y}=0, \tag{18}$$

where W and A are the material fluid parameters. Note that the continuity equation is identically satisfied and the shape of peristaltic wall $h(x)$ in dimensionless form is given by

$$h(x)=1+\phi\ \sin x, \tag{19}$$

in which $\phi\,(=b/d)$ is the amplitude ratio with $0<\phi<1$. The flow rate in fixed frame is

$$\bar{Q}=\int_0^{\bar{h}}(\bar{u}+c)\,d\bar{y}=\int_0^{\bar{h}}\bar{u}d\bar{y}+\int_0^{\bar{h}}cd\bar{y}=q+c\bar{h}. \tag{20}$$

The average volume flow rate over one period $\left(T=\frac{\lambda}{c}\right)$ of the peristaltic wave is defined as follows:

$$Q=\frac{1}{T}\int_0^T\bar{Q}d\bar{t}=\frac{1}{T}\int_0^T\left(q+c\bar{h}\right)d\bar{t}=q+cd.$$
$$\Theta=F+1. \tag{21}$$

In above equation $\Theta\left(=\frac{Q}{cd}\right)$ and $F\left(=\frac{q}{cd}\right)$ are the dimensionless time-mean flow rates in the fixed and wave frames, respectively. The relevant boundary conditions with respect to wave frame are

$$\Psi=0,\qquad \frac{\partial^2\Psi}{\partial y^2}=0,\qquad at\ y=0, \tag{22}$$

$$\frac{\partial\Psi}{\partial y}=-1-\alpha\mathbf{S}_{xy},\quad \Psi=F,\quad at\ y=h, \tag{23}$$

where α is the slip parameter, $\mathbf{S}_{xy}$ is the dimensionless shear stress and

$$F=\int_0^h\frac{\partial\Psi}{\partial y}dy=\Psi(h)-\Psi(0). \tag{24}$$

The expressions of non-dimensional pressure rise per wavelength ($\triangle P_\lambda$) is

$$\triangle P_\lambda = \int_0^{2\pi} \frac{dp}{dx} dx, \tag{25}$$

3. Development of series solution

Equations (15)–(17) are non-linear and closed form solutions of these equations seem difficult. Therefore we will seek perturbation solution by considering fluid parameter A as a perturbation parameter and expand Ψ, F and p in the forms:

$$\Psi = \Psi_0 + A\ \Psi_1 + A^2\Psi_2, \tag{26}$$

$$F = F_0 + A\ F_1 + A^2 F_2, \tag{27}$$

$$p = p_0 + A\ p_1 + A^2 p_2. \tag{28}$$

Using above relations and setting $F_0 = F - AF_1 - A^2F_2$, one has the following resulting expressions:

$$\begin{aligned}
\Psi(y) = {} & \frac{y}{2h^2(h+3(1+W)\alpha)}(h^3 - hy^2 \\
& +F(-y^2 + 3h(h+2(1+W)\alpha))) \\
& -(\frac{A}{20h^6(1+W)(h+3(1+W)\alpha)^4}) \\
& 27(F+h)^3(hy(h^2-y^2)^2 \\
& +3y(1+W)(y^4-h^4)\alpha) \\
& -(\frac{A^2}{700h^{10}(1+W)^2(h+3(1+W)\alpha)^7}) \\
& 243y(F+h)^5(h^2-y^2)(h^2(h^2 \\
& -y^2)(37h^2+50y^2) + 3h(1+W)(113h^4 \\
& -37h^2y^2 - 100y^4)\alpha - 450(1+W)^2 \\
& (h^4+h^2y^2+y^4)\alpha^2)),
\end{aligned}$$

$$\frac{dp}{dx} = -\frac{3(F+h)(1+W)}{h^2(h+3(1+W)\alpha)} + \frac{81A(F+h)^3}{5h^3(h+3(1+W)\alpha)^4} \frac{2187A^2(F+h)^5\,(4h+75(1+W)\alpha)}{175h^5(1+W)(h+3(1+W)\alpha)^7}.$$

4. Graphical results

In this section we discuss the effect of emerging parameters on the flow. For this purpose, we divided

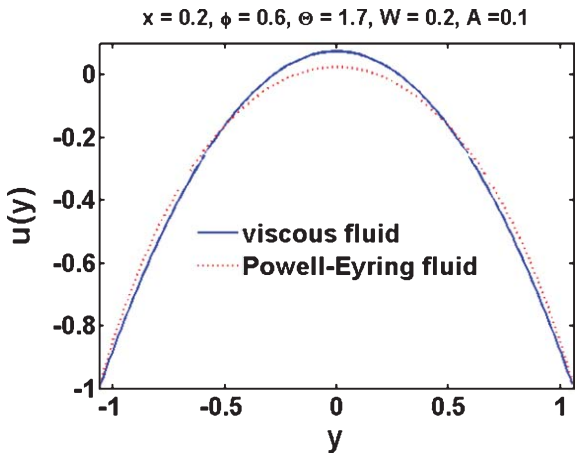

Fig. 1. Comparison of vicous and Powell-Erying fluids for $u(y)$.

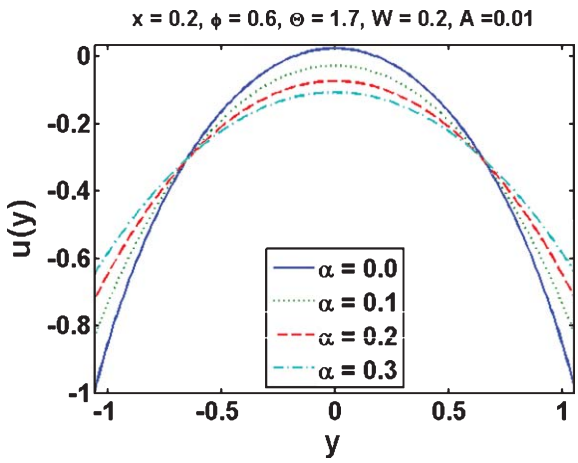

Fig. 2. Variation in $u(y)$ against y for different values of slip parameter (α).

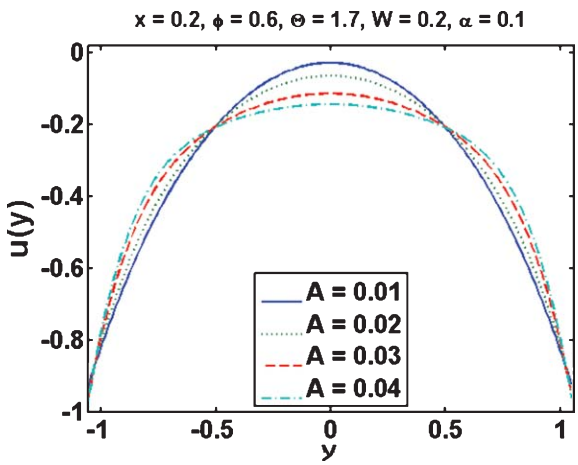

Fig. 3. Variation in $u(y)$ against y for different values of fluid parameter (A).

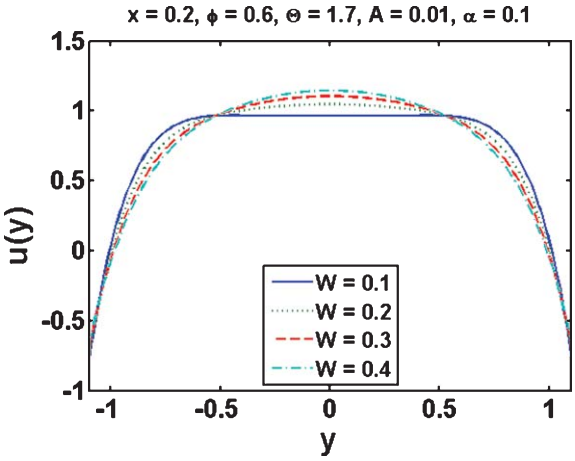

Fig. 4. Variation in $u(y)$ against y for different values of fluid parameter (W).

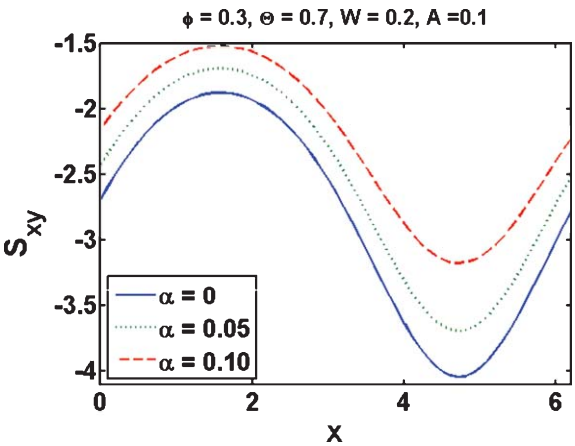

Fig. 5. Variation in shear stress (S_{xy}) against y for different values of slip parameter (α).

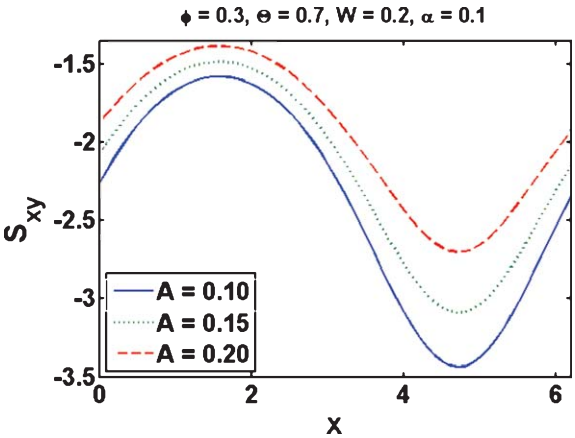

Fig. 6. Variation in shear stress (S_{xy}) against y for different values of fluid parameter (A).

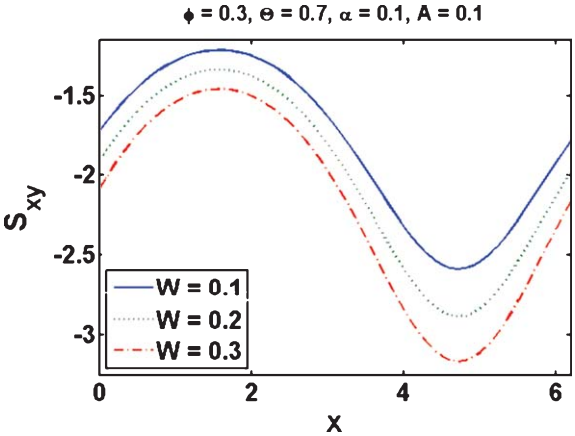

Fig. 7. Variation in shear stress (S_{xy}) against y for different values of fluid parameter (W).

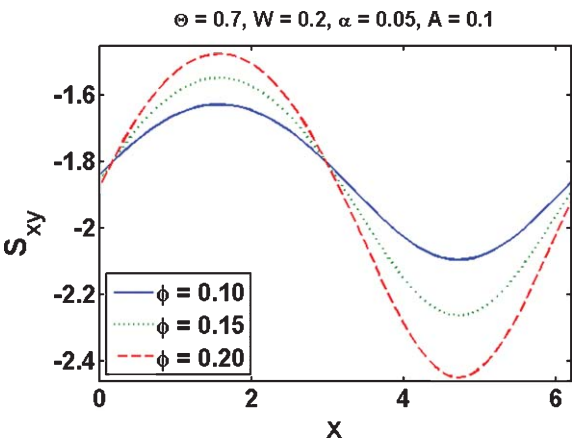

Fig. 8. Variation in shear stress (S_{xy}) against y for different values of amplitude ratio (ϕ).

the section into four subsections. In subsection one we displayed the effect of pertinent flow parameters on the velocity profile, subsection two presents the influence of flow parameters on the axial shear stress (S_{xy}). Plots in subsection three display the effect of pressure gradient $\left(\frac{dp}{dx}\right)$. Subsection four displays the effect for pressure rise (ΔP_λ) and finally effect of flow parameters on the trapping is analyzed in subsection five.

4.1. Velocity profile

In Fig. 1 a comparison between viscous fluid and non-Newtonian Powell-Eyring fluid is presented by neglecting the slip effect ($\alpha = 0$) through axial

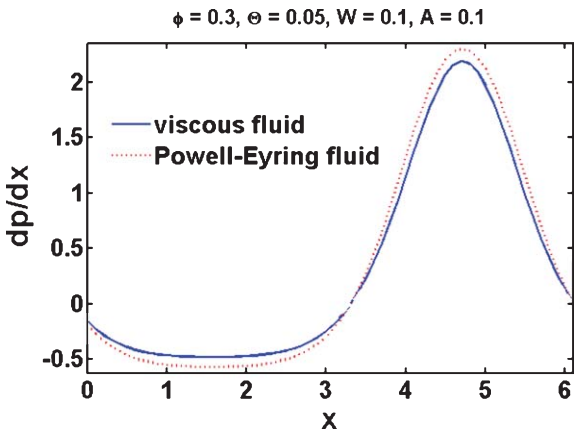

Fig. 9. Comparison of viscous and Powell-Erying fluids for dp/dx.

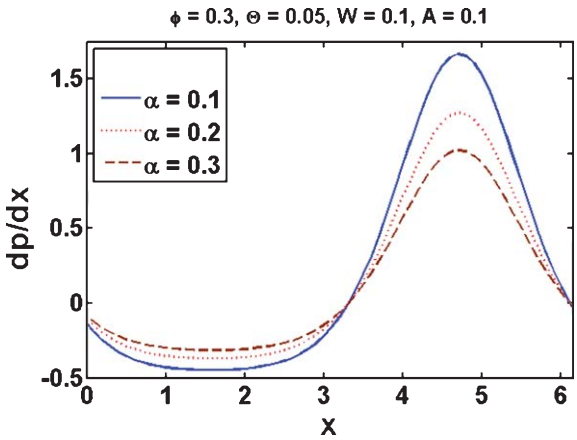

Fig. 10. Variation in dp/dx against x for different values of slip parameter (α).

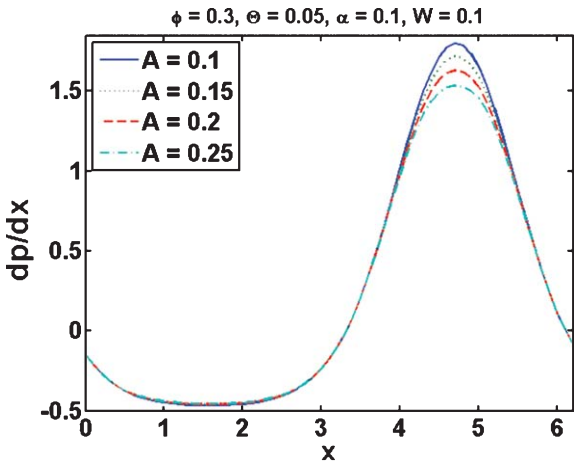

Fig. 11. Variation in dp/dx against x for different values of fluid parameter (A).

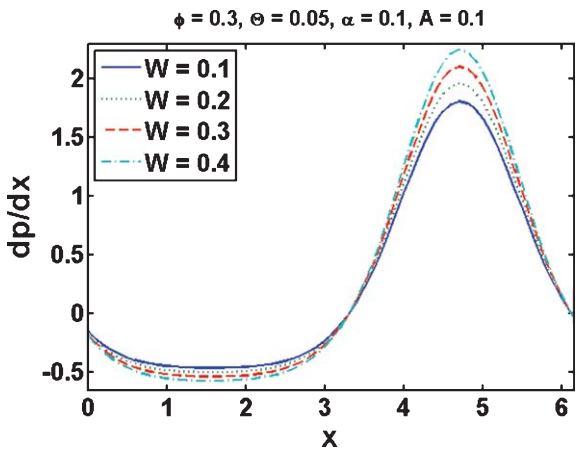

Fig. 12. Variation in dp/dx against x for different values of fluid parameter (W).

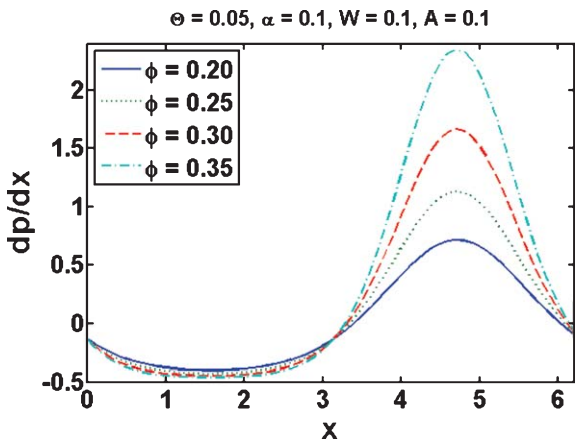

Fig. 13. Variation in dp/dx against x for different values of amplitude ratio (ϕ).

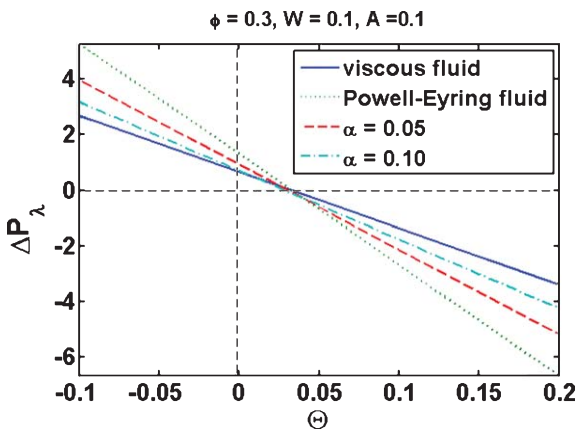

Fig. 14. Variation in ΔP_λ against Θ for different values of slip parameter (α).

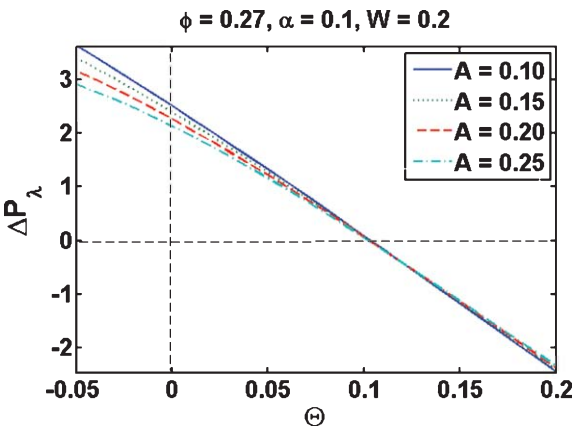

Fig. 15. Variation in ΔP_λ against Θ for different values of fluid parameter (A).

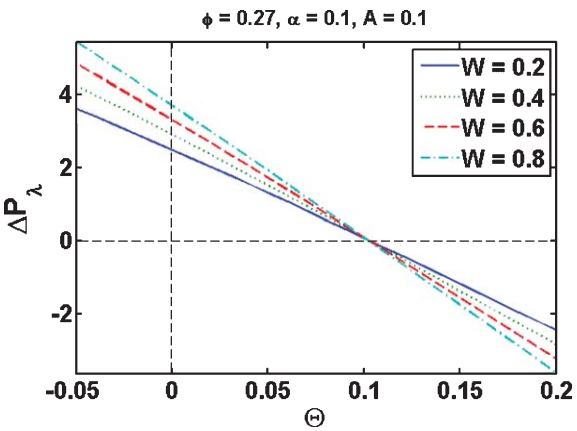

Fig. 16. Variation in ΔP_λ against Θ for different values of fluid parameter (W).

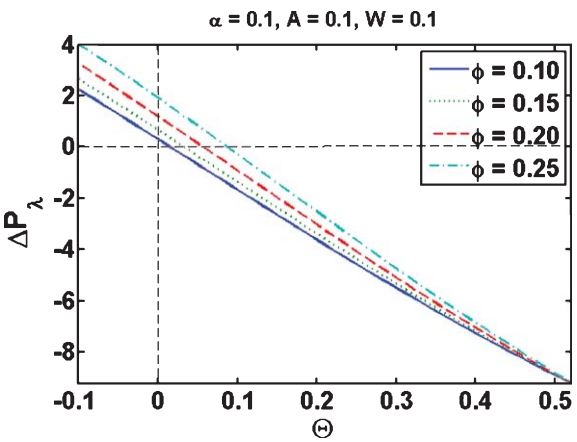

Fig. 17. Variation in ΔP_λ against Θ for different values of amplitude ratio (ϕ).

velocity. The plots reflect that the velocity for viscous fluid is greater than Powell-Eyring fluid at the central of channel. However the situation is opposite near the walls. Influence of slip parameter (α) on the velocity is displayed in Fig. 2. It is found that by increasing α, the velocity of fluid at the central part of the channel decreases whereas it increases near the walls of the channel. Effect of fluid parameters (A) and (W) is presented in Figs. 3 and 4. The effect of these parameters on the flow is qualitatively opposite to each other. Increase in A decreases the velocity of the fluid at the central part of the channel while increase in W enhances the fluid velocity near the center of channel.

4.2. Shear stress at the wall

In this subsection Figs. (5–8) are displayed to analyze the effect of α, A, W and amplitude ratio ϕ on the axial shear stresses $\left(S_{xy}\right)$ at the wall $y = h$. Fig. 5 reflects that by increasing slip parameter α the magnitude of shear stress decreases. Influence of fluid parameters A and W on shear stress are presented in Figs. 6 and 7. It is noted that effects of A and W are opposite to each other. Absolute value of stress decreases for an increase in A while the magnitude of shear stresses increases for increasing values of W. Effect of amplitude ratio ϕ on the shear stress is plotted in Fig. 8. The plots depict that by increasing ϕ the magnitude of the stresses decrease in the wider part of channel for $0 < x < \pi$ while the magnitude of shear stress increases in the narrow part of the channel $\pi < x < 2\pi$.

4.3. Pressure gradient

This subsection analyze the influence of slip parameter (α) , material parameters (A and W) and amplitude ratio (ϕ) on the pressure gradient in Figs. (9–13). These plots reflect that in the wider part of the channel ($0 < x < \pi$) the pressure gradient is relatively small and the flow can easily pass without imposition of large pressure gradient. However in narrow part of the channel ($\pi < x < 2\pi$) a much larger pressure gradient is required to maintain the same flux to pass through it. Figure 9 presents a comparison between viscous and powell-Eyring fluids. A comparative study indicates that the magnitude of pressure gradient for Powell-Eyring fluid is greater than viscous fluid in the narrow part of the channel. Plot in Fig. 10 is prepared to

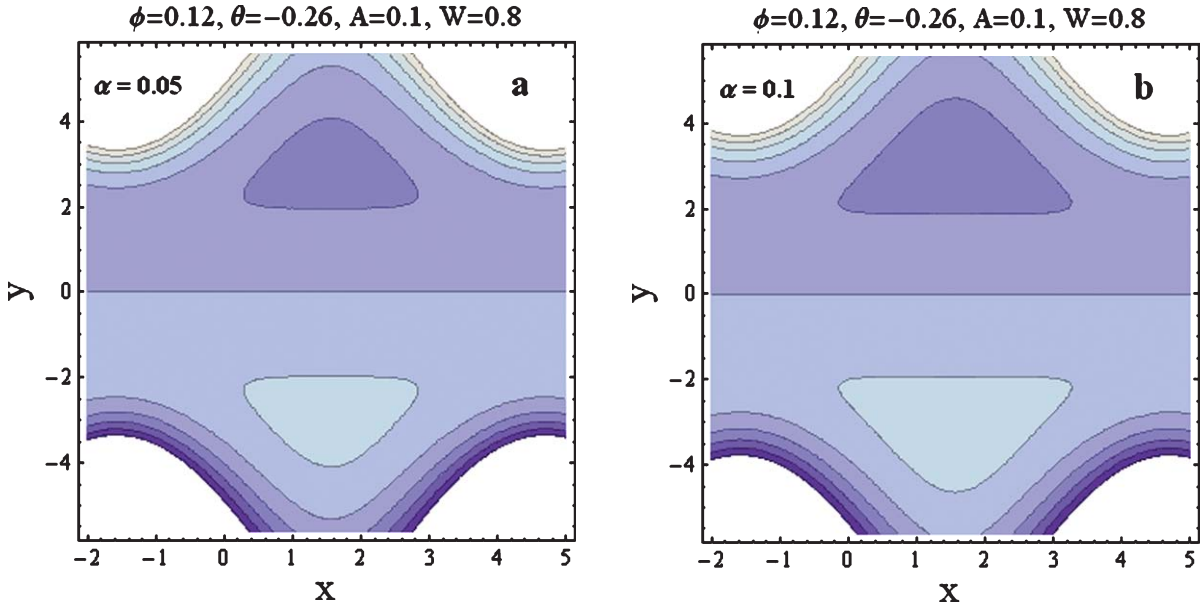

Fig. 18. (a,b) Plots of stream lines for different values of slip parameter (α).

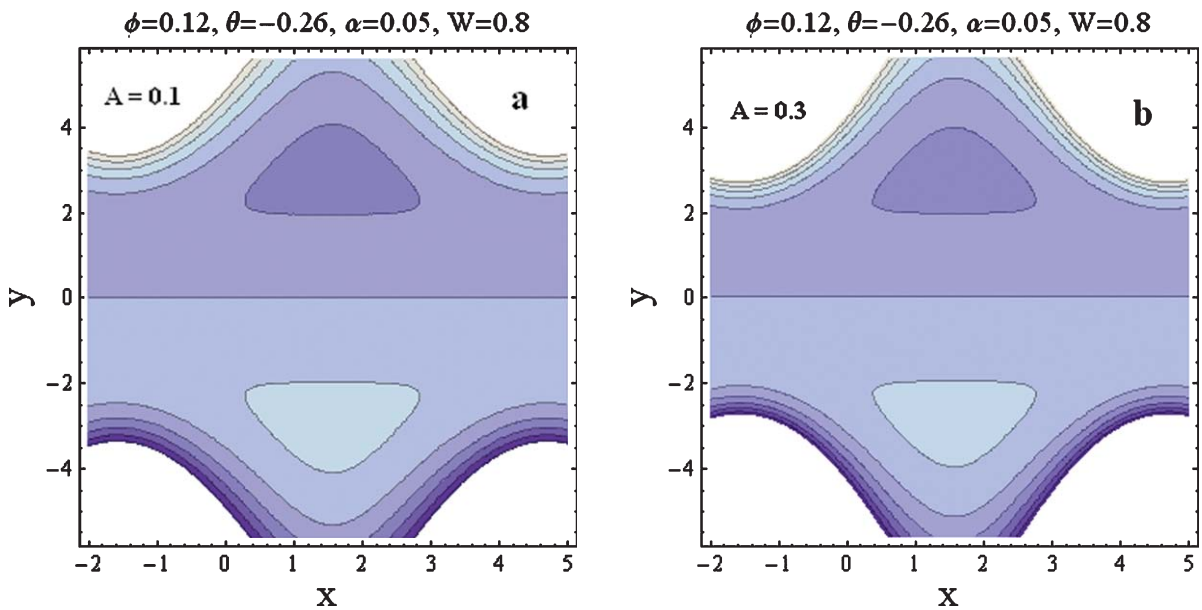

Fig. 19. (a,b) Plots of stream lines for different values of fluid parameter (A).

illustrate the effect of slip parameter (α) on the axial pressure gradient. It is abserved that the magnitude of pressure gradient decreases by increasing α in the narrow part of the channel. Effect of material parameters A and W on pressure gradient are displayed in the Figs. 11 and 12. These plots depict that the effect of both parameters A and W are quite opposite i.e. by increasing A the pressure gradient decreases while the magnitude of the pressure gradient increases for larger W. Impact of amplitude ratio (ϕ) on pressure gradient is

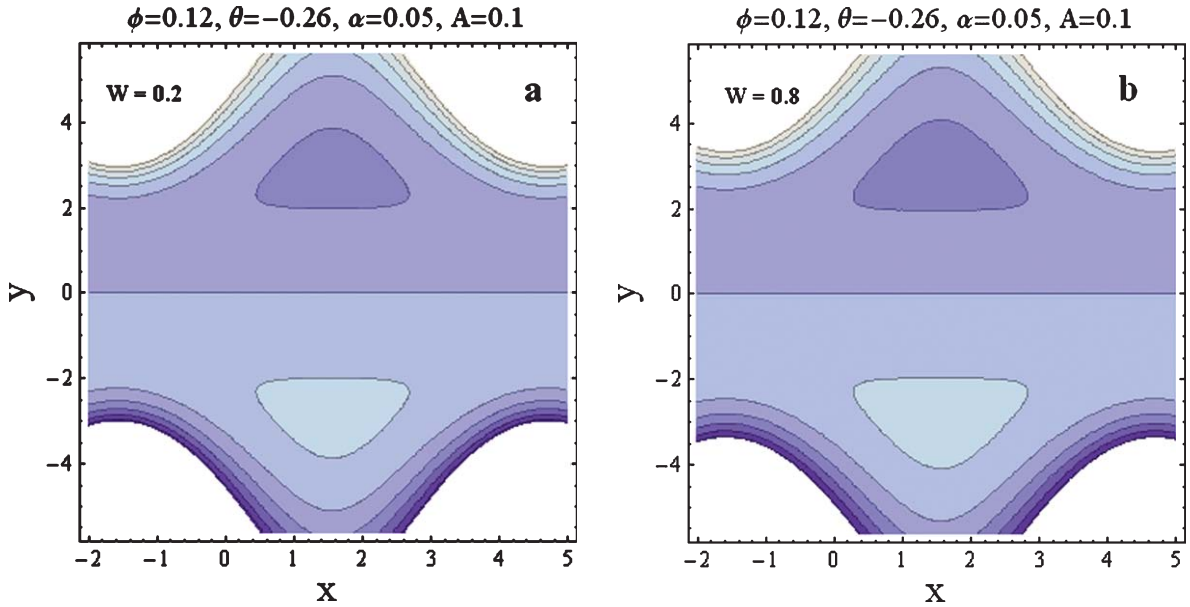

Fig. 20. (a,b) Plots of stream lines for different values of fluid parameter (W).

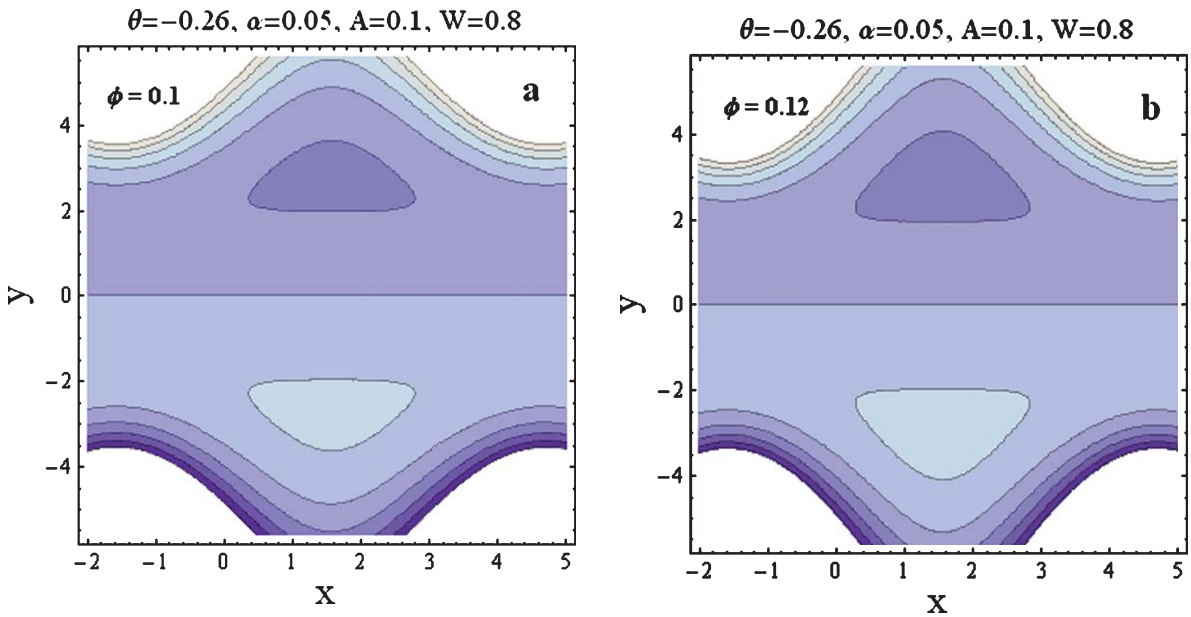

Fig. 21. (a,b) Plots of stream lines for different values of amplitude ratio (ϕ).

presented in Fig. 13. The plot shows that the magnitude of pressure gradient increases when ϕ enhances.

4.4. Pressure rise

Figures (14–17) are displayed to examine the variation of dimensionless pressure rise (ΔP_λ) versus the time-average flux (Θ) for various values of pertinent flow parameters. For that numerical integration is performed through Equation (15) . The graphs are sectored so that the upper right-hand quadrant that is $\Theta > 0$ and $\Delta P_\lambda > 0$ represents the peristaltic pumping region while the lower left hand quardant for $\Theta > 0$ and $\Delta P_\lambda < 0$ is designated as augmented pumping region.

These plots show a linear relation between ΔP_λ and Θ. Figure 14 is prepared to analyze the effect of slip parameter (α) on ΔP_λ. It is noted that pressure rise decreases with an increase in α. Furthermore a comparison for visous and Powell-Eyring fluids is also presented in Fig. 14. This figure shows that the value of pressure rise for Powell-Eyring fluid is greater than that of viscous fluid. Influence of material fluid parameters A and W on ΔP_λ are illustrated in Figs. 15 and 16. The behaviors of A and W on pressure rise are opposite to each other i.e. an increase in material parameter A decreases the pressure rise while pressure rise increases by increasing W in the peristaltic pumping region. Plot in Fig. 17 presents the effect of amplitude ratio (ϕ) on pressure rise. It is noted that an increase in ϕ enhances the pressure rise.

4.5. Trapping

The effect of slip parameter (α), material fluid parameters (A and W) and amplitude ratio (ϕ) on trapping can be seen through Figs. (18) − (21). These plots depict that the size of the trapped bolus increases with an increase in slip parameter α, material parameter W and amplitude ratio ϕ. However the size of the bolus decreases for increasing values of material parameter A.

5. Conclusions

In the present paper, we have analyzed the partial slip effect on peristaltic flow of Powell-Eyring fluid in a symmetric channel. The differential system has been modeled and then simplified using long wavelength approximation. The results are discussed through graphs. We have the following main observations.

- The velocity decreases for the slip parameter (α) and fluid parameter (A) at the centre of the channel. However effect of fluid parameters (W) on the velocity profile is opposite to both α and A. The velocity profile shows an opposite behavior near the channel walls when compared with the channel centre.
- Magnitude of axial shear stress decreases for slip parameter (α) and material parameter (A). However the magnitude of axial shear stress increases for material parameter (W).
- Pressure gradient decreases for slip parameter (α) and material parameter (A). However pressure gradient increases with an increase in fluid parameter (W) and amplitude ratio (ϕ).
- Pressure rise increases in peristaltic pumping region for an increase in slip parameter (α), material parameter (W) and amplitude ratio (ϕ). The effect of material parameter (A) is to decrease the pressure rise.
- The size of trapped bolus decreases for an increase in fluid parameter (A). However opposite effects are noted for slip parameter (α), fluid parameter (W) and amplitude ratio (ϕ) for the size of the trapped bolus.

References

[1] T.W. Latham, *Fluid motion in a peristaltic pump*, MS. Thesis, M.I.T. Cambridge, (1966).

[2] A.H. Shapiro, M.Y. Jaffrin and S.L. Weinberg, Peristaltic pumping with long wave lengths at low Reynolds numbers, *J Fluid Mech* **37** (1969), 99–825.

[3] H. L. Agrawal and B. Anwaruddin, Peristaltic flow of blood in a branch, *Ranchi University Math J* **15** (1984), 111–125.

[4] L.M. Srivastava and V.P. Srivastava, Peristaltic transport of a power-law fluid: Application to the ductus efferentes of the reproductive tract, *Rheologica Acta* **27** (1988), 428–433.

[5] M. Mishra and A.R. Rao, Peristaltic transport of a Newtonian fluid in an asymmetric channel, *Z Angew Math Phys* **54** (2003), 532–550.

[6] Kh. S. Mekheimer and Y. Abd elmaboud, Peristaltic flow through a porous medium in an annulus: Application of an endoscope, *Appl Math Inform Sci* **2** (2008), 103–111.

[7] T. Hayat, S. Hina, A.A. Hendi and S. Asghar, Effect of wall properties on the peristaltic flow of a third grade fluid in a curved channel with heat and mass transfer, *Int J Heat Mass Trans* **54** (2011), 5126–5136.

[8] S.K. Pandey and M.K. Chaube, Study of wall properties on peristaltic transport of a couple stress fluid, *Meccanica* **46** (2011), 1319–1330.

[9] D. Tripathi, A mathematical model for the peristaltic flow of chyme movement in small intestine, *Math Bio Sci* **233** (2011), 90–97.

[10] Kh. S. Mekheimer and A.N. Abdel-Wahab, Net annulus flow of a compressible viscous liquid with peristalsis, *J Aerosp Eng* **25** (2012), 660–669.

[11] P. Lakshminarayana1, S. Sreenadh and G. Sucharitha, Peristaltic pumping of a conducting fluid in a channel with a porous peripheral layer, *Adv Appl Sci Res* **3** (2012), 2890–2899.

[12] S. Maiti and J.C. Misra, Non-Newtonian characteristics of peristaltic flow of blood in micro-vessels, *Commun Nonlinear Sci Numer Simulat* **18** (2013), 1970–1988.

[13] M.M. Rashidi, T. Hayat, E. Erfani, S.A. Mohimanian Pour and A.A. Hendi, Simultaneous effects of partial slip and thermal-diffusion and diffusion-thermo on steady MHD convective

flow due to a rotating disk, *Commun Nonlinear Sci Numer Simulat* **16** (2011), 4303–4317.

[14] M.M. Rashidi, S. Abelman and N.F. Mehr, Entropy generation in steady MHD flow due to a rotating porous disk in a nanofluid, *Int J Heat Mass Trans* **62** (2013), 515–525.

[15] M.M. Rashidi, M. Ali, N. Freidoonimehr and F. Nazari, Parametric analysis and optimization of entropy generation in unsteady MHD flow over a stretching rotating disk using artiÖcial neural network and particle swarm optimization algorithm, *Energy*, **55** (2013), 497–510.

[16] N. Ali, Q. Hussain, T. Hayat and S. Asghar, Slip effects on the peristaltic transport of MHD fluid with variable viscosity, *Phys Lett A* **372** (2008), 1477–1489.

[17] S. Srinivas, R. Gayathri and M. Kothandapani, The influence of slip conditions, wall properties and heat transfer on MHD peristaltic transport, *Comp Phy Commun* **180** (2009), 2115–2122.

[18] A. Yıldırım and S.A. Sezer, Effects of partial slip on the peristaltic flow of a MHD Newtonian fluid in an asymmetric channel, *Math Comput Model* **52** (2010), 618–625.

[19] T. Hayat, Q. Hussain, M.U. Qureshi, N. Ali and Awatif A. Hendi, Influence of slip condition on the peristaltic transport in an asymmetric channel with heat transfer: An exact solution, *Int J Numer Meth Fluids*, **67** (2011), 1944–1959.

[20] D. Tripathi, P.K. Gupta and S. Das, Influence of slip condition on periataltic transport of a viscoelastic fluid with fractional Burgers' model, *Thermal Science*, **15** (2011), 501–515.

[21] N.S. Akbar, T. Hayat, S. Nadeem and S. Obaidat, Peristaltic flow of a Williamson fluid in an inclined asymmetric channel with partial slip and heat transfer, *Int J Heat Mass Trans* **55** (2012), 1855–1862.

[22] A. Afsar Khan, R. Ellahi and M. Usman, Effects of variable viscosity on the flow of non-Newtonian fluid through a porous medium in an inclined channel with slip conditions, *J Porous Media* **16** (2013), 59–67.

[23] T. Hayat and O.U. Mehmood, Slip effects on MHD flow of third order fluid in a planar channel, *Commun Nonlinear Sci Numer Simulat* **16** (2011), 1363–1377.

[24] K. Vajravelu, S. Sreenadh and R. Saravana, Combined influence of velocity slip, temperature and concentration jump conditions on MHD peristaltic transport of a Carreau fluid in a non-uniform channel, *Appl Math comp* **225** (2013), 656–676.

[25] R.E. Powell and H. Eyring, Mechanism for the relaxation theory of viscosity, *Nature*, **154** (1944), 427–428.

[26] T. Hayat, Z. Iqbal, M. Qasim and S. Obaidat, Steady flow of an eyring powell fluid over a moving surface with convective boundary conditions, *Int J Heat Mass Transfer*, **55** (2012), 1817–1822.

[27] T. Hayat and M. Farooq, Melting heat transfer in the stagnation point flow of Powell-Eyring fluid, *J Thermophys Heat Trans* **27** (2013), 761–766.

[28] T. Hayat, M. Awais and S. Asghar, Radiative effects in a three-dimensional flow of MHD Eyring-Powell fluid, *J Egyp Math Soc* **21** (2013), 379–384.